Molecular Diversity (2021) 25:787–799
https://doi.org/10.1007/s11030-020-10057-7

ORIGINAL ARTICLE

Hydrazine clubbed 1,3-thiazoles as potent urease inhibitors: design, synthesis and molecular docking studies

Pervaiz Ali Channar[1] · Aamer Saeed[1] · Saira Afzal[2] · Dilawar Hussain[2] · Markus Kalesse[4] · Syeda Aaliya Shehzadi[3] · Jamshed Iqbal[2]

Received: 29 November 2019 / Accepted: 17 February 2020 / Published online: 24 February 2020

Abstract

Synthesis of a novel series of hydrazine clubbed 1,3-thiazoles (**5a–m**) has been described by reacting hydrazine-1-carbothioamides (**3a–k**) with α-chloro- or bromo-acetophenones (**4a–d**) in refluxing ethanol in good to excellent yields (65–86%). Structural confirmation was based upon spectroscopic techniques such as ^{1}H-NMR, ^{13}C-NMR, FT-IR and mass spectrometry. The biological application of these motifs has been demonstrated in terms of their strong urease inhibition activity. The results of in vitro study revealed that all the compounds are the potent inhibitors of urease. The IC_{50} (ranging in between 110 and 440 nM) values were higher as compared to that of standard, i.e., thiourea ($IC_{50} = 490 \pm 10$ nM). The synthesized compounds were docked at the active sites of the Jack bean urease enzyme in order to explore the possible binding interactions of enzyme–ligand complexes; the results reinforced the in vitro biological activity results.

Graphic abstract

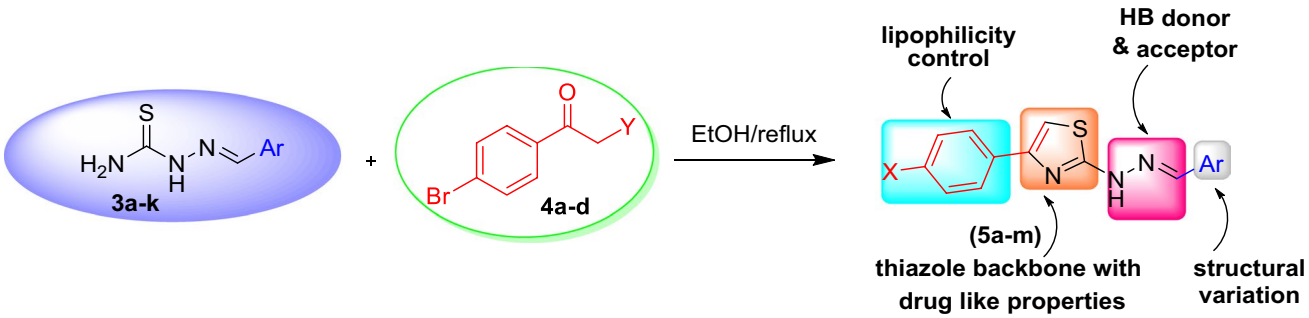

Keywords Hydrazine-1,3-thiazole · Urease inhibition · Molecular docking

Electronic supplementary material The online version of this article (https://doi.org/10.1007/s11030-020-10057-7) contains supplementary material, which is available to authorized users.

✉ Aamer Saeed
aamersaeed@yahoo.com

✉ Jamshed Iqbal
drjamshed@cuiatd.edu.pk

[1] Department of Chemistry, Quaid-i-Azam University, Islamabad 45320, Pakistan

[2] Centre for Advanced Drug Research, COMSATS University Islamabad, Abbottabad Campus, Abbottabad 22060, Pakistan

[3] Sulaiman Bin Abdullah Aba Al-Khail-Centre for Interdisciplinary Research in Basic Sciences (SA-CIRBS), International Islamic University, Islamabad 44000, Pakistan

[4] Institut für Organische Chemie, Schneiderberg 1B, 30167 Hannover, Germany

Introduction

The dangerous buildup of large amounts of urea in the body by catabolism of proteins can cause uremia resulting in metabolic acidosis leading to high blood pressure, swelling and other skin problems. Hydrolysis of urea produces ammonia and carbamic acid, and the latter further breaks down into more ammonia and carbon dioxide [1, 2]. Nature performs this hydrolysis by a nickel containing enzyme called urease (urea aminohydrolase E.C.3.5.1.5) that catalyzes the hydrolysis of urea at a rate approximately 10^{14} times higher than the rate of an un-catalyzed reaction [3–5]. Mammalian cells do not produce urease; however, urease is found in mammals and the sources are the various bacteria. The urease activity also leads to certain medical implications such as ammonia encephalopathy, appearance of urinary stones, catheters blocking, pyelonephritis and hepatic coma [6]. Certain bacterial urease causes stomach cancer and peptide ulceration [7, 8]. Therefore, this enzyme is the main target of the biochemists, physiologists and medicinal chemists [9–11] and various strategies have been adopted to treat diseases caused by bacterial ureases by inhibiting its activity.

Several literature reviews report the application of heterocycles as promising scaffolds to cure urease-generated problems [12–14]. In particular, thiazoles are the most potent candidates for the anti-urease activity [15]. Thiazole is the vital part of numerous drug structures such as dasatinib [16], ritonavir [17, 18], ravuconazole [19, 20], fanetizole [21], nizatidine [22] sulfathiazole and tiazofurin [23, 24] are some examples of thiazole bearing drugs in the market.

On the other hand, hydrazinyl derivatives are some of the most widely used organic compounds exhibit a broad range of biological activities. The attachment of hydrazinyl group confers extra biological potential to various heterocycles. Thus, hydrazinyl thiazolyl coumarins exhibit cytotoxicity, antibacterial, antitubercular activities, 2-(2-hydrazinyl)thiazole derivatives vitro antimycobacterial and arylidene-hydrazinyl-thiazole and arylidene-hydrazinyl-thiazole derivatives antiproliferative activities [25–29]. Figure 1 shows structures of some bioactive molecules with 1,3-thiazole and hydrazinyl linkages.

In this viewpoint, due to the significant relevance of thiazole derivatives in medicinal chemistry, we focused to explore their urease inhibition potential and the outcomes are described in the results and discussion section of this article.

Results and discussions

Chemistry

The synthesis of hydrazinyl-thiazole derivatives (**5a–m**) was carried out in two steps. In the first step, suitably substituted benzaldehydes (**2a–k**) were treated with an equimolar quantity of thiosemicarbazide (**1**) in ethanol in the presence of a few drops of glacial acetic acid. The pure (aryl)methylene) hydrazine-1-carbothioamides (**3a–k**) products were obtained by recrystallization from methanol in good yields. Heterocyclization of the latter with an equimolar quantity of appropriate α-haloacetophenones (**4a–d**) afforded the hydrazinyl-1,3-thiazoles (**5a–m**) as pure products in high yields as shown in Scheme 1. A variety of aldehydes including heterocyclic, aromatic and polycyclic aromatic ones were for the structural variation in designed thiazole derivatives (**5a–m**) to develop structure activity relationship.

In ^{1}H-NMR, of thiosemicarbazones (**3a–k**), the most deshielded N–H proton resonated around δ11–12 ppm, while the characteristic proton of sp^2 hybridized carbon (HC=N) appeared at 7.9–9.3 ppm. The thiazole ring formation was confirmed by typical one proton singlet in the aromatic region due to being attached with a sp^2 carbon and sulfur atom. In the ^{13}C-NMR spectra of the condensation product (**3a–k**), a distinguishing azomethine carbon appeared at 165 ppm value. In the thiazole compounds (**5a–m**), the carbon directly attached to nitrogen appeared around δ166–178 ppm. The signals in the range 140 to 120 ppm belong to aromatic carbons and the carbon directly linked with oxygen appeared at 55–60 ppm in case of compounds **5a**, **5b** and **5l**.

Structure activity relationship (SAR)

A series of 11 hydrazine clubbed 1,3-thiazoles (**5a–i** and **5k–l**) was evaluated for inhibition of urease. All these compounds were found to be very potent inhibitors of urease with IC_{50} values ranging from 110 to 440 nM, whereas the IC_{50} value of standard inhibitor, i.e., thiourea was 490 ± 10 nM. These compounds were substituted with different functional groups at the nitrogen atom of hydrazine. Moreover, the position 4 of the thiazole ring contained either a bromo- or chlorophenyl moiety attached to it (Table 1).

The highest inhibitory activity was shown by compound **5i** (110 ± 3 nM) and **5l** (110 ± 5 nM). Interestingly, both of these compounds had an equal IC_{50} value. A detailed structural analysis revealed that these compounds contained substituted benzylidene ring as structural variant with electron donating groups. In case of **5i**, a methyl group was present at C-4 of benzylidene ring. However, the compound **5l** was substituted with three methoxy groups at C-3, -4 and -5 of the benzylidene ring. Thus, the activity of these compounds might be attributed to the presence of the electron donating groups. A comparison of **5i** and **5l** with **5k** further supports this hypothesis, since compound **5k** contained two electron withdrawing groups, i.e., NO_2 and Cl attached to it and the activity of **5k** was 2.5 times lower as compared to **5l** and **5i** (Fig. 2).

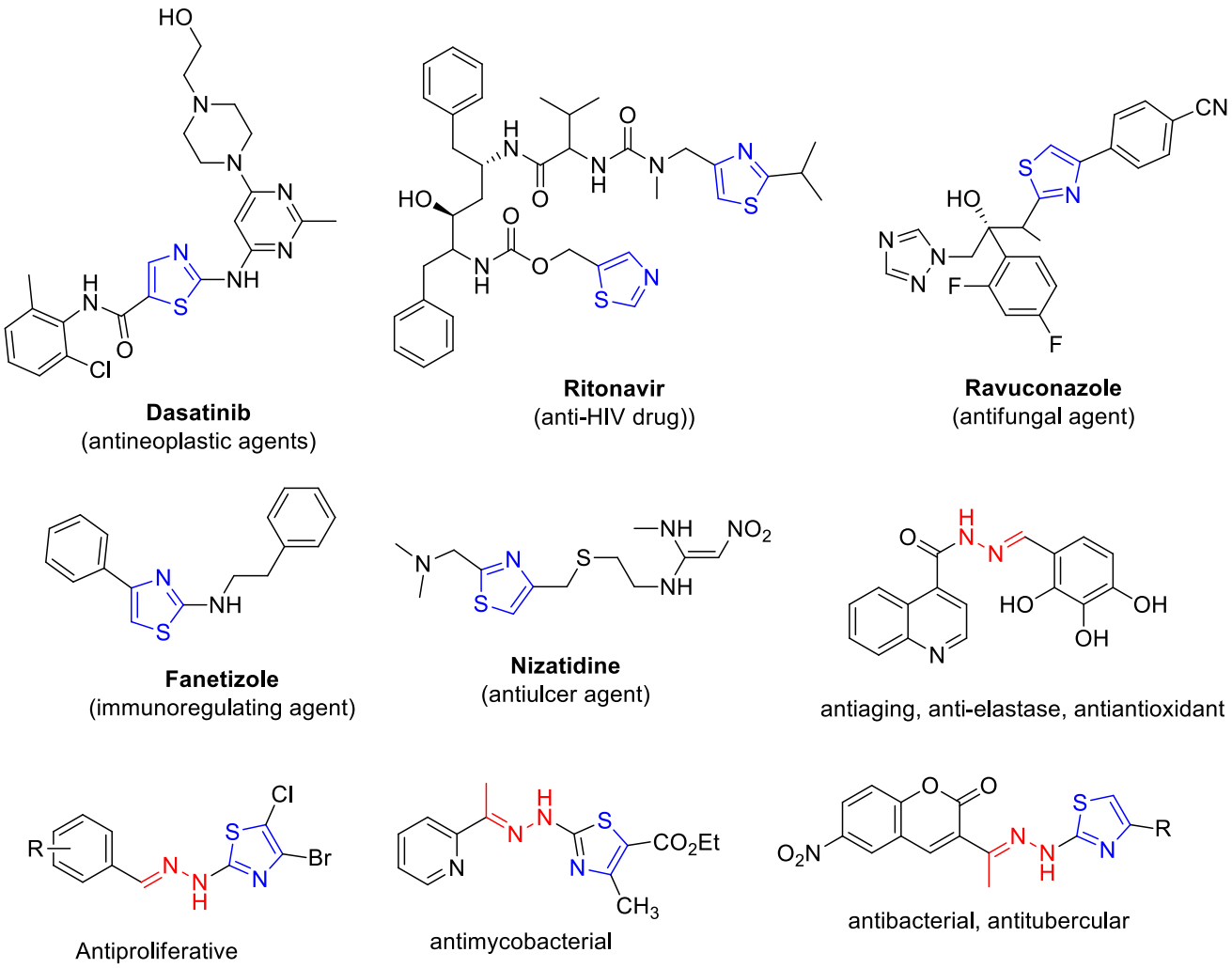

Fig. 1 Examples of bioactive molecules with 1,3-thiazole and hydrazinyl linkages

However, the introduction of benzyloxy group to the benzylidene ring appeared to be less favorable as reflected by the IC_{50} values of **5a** (330 ± 30 nM) and **5b** (440 ± 20 nM). Although this benzyloxy group was an electron donating group, its bulky nature could be responsible for the reduced activity. In this context, the IC50 value of 5a is considerably high as compared to that of **5b**, although there is slight difference in their structure. The compound 5a contains a methoxy group on the benzene ring, in addition to benzyloxy group. It can be suggested that, here, this methoxy group is acting as electron withdrawing group. Thus, it might withdraw the electrons inductively and leading to the enhanced activity of compound **5a** than that of **5b** (Fig. 3).

Moreover, different heterocyclic rings were also attached to the hydrazine via CH bond. Among these compounds, a definite pattern of activity was observed, and they inhibited the urease in the following order of activity.

Furan (**5f**, IC_{50} = 120 ± 3 nM) > thiophene (**5h**, IC_{50} = 130 ± 2 nM) > pyridine (**5c**, IC_{50} = 160 ± 4 nM) > pyrrole (**5g**, IC_{50} = 200 ± 2 nM).

However, it was worth mentioning that thiophene and pyrrole rings were substituted with bromine. Thus, the substitution might also be a contributing factor to this pattern of inhibition activity (Fig. 4).

In this regard, a comparison of **5g** and **5h** is of particular importance. Both of these compounds contain bromophenyl ring attached to thiazole ring, whereas the hydrazine is attached to five-membered heterocyclic ring. In case of **5g**, 5-bromo-pyrrole was present, whereas **5h** contained 5-bromo-thiophene. However, compound **5h** (IC_{50} = 130 ± 2 nM) had better activity as compared to **5g** (IC_{50} = 200 ± 2 nM). This enhanced activity of **5g** could be assigned to the presence of thiophene ring since sulfur atom would be involved in sulfur–pi bonding within the active pocket of enzyme. The 4-chlorophenyl and

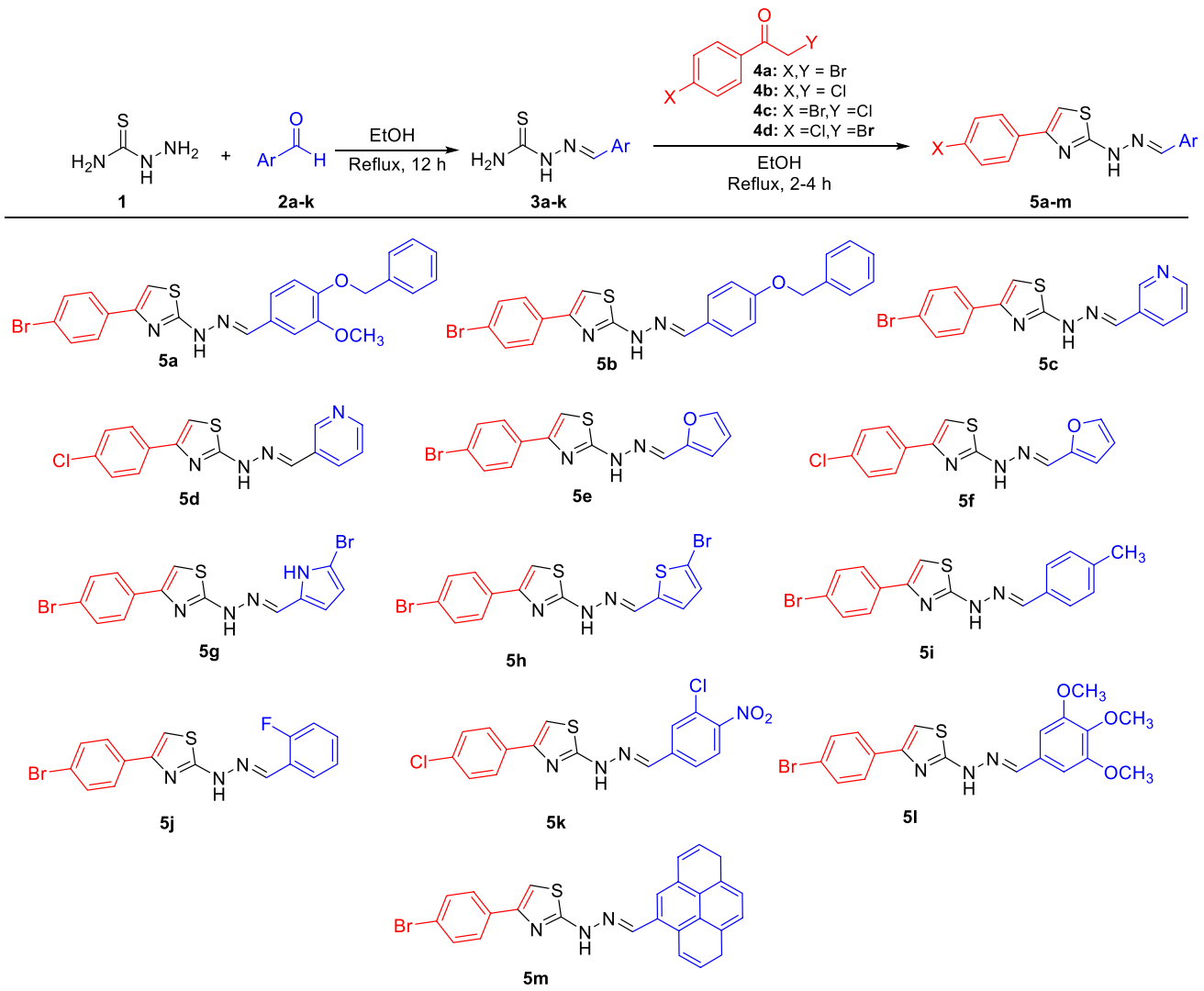

Scheme 1 Synthesis of hydrazinyl-1,3-thiazole derivatives **(5a–m)**

Table 1 Urease inhibitory activity of hydrazinyl-thiazole derivatives

Compound	IC_{50} (nM) ± SEM
5a	330 ± 30
5b	440 ± 20
5c	160 ± 4
5d	260 ± 20
5e	210 ± 10
5f	120 ± 3
5g	200 ± 2
5h	130 ± 2
5i	110 ± 3
5k	280 ± 10
5l	110 ± 5
Thiourea	490 ± 10

4-bromophenyl group attached to basic thiazole nucleus influenced the inhibitory activity as well. For example, a comparison of the IC_{50} values of **5e** vs **5f** revealed that the furan ring was best suited with 4-chlorophenyl (**5f,** $IC_{50} = 120 \pm 3$ nM) as compared to 4-bromophenyl (**5e**, $IC_{50} = 210 \pm 10$ nM) (Fig. 5).

Conversely, a reverse trend was observed in case of pyridine ring, where **5c** (containing 4-bromophenyl ring) was 1.6-fold more potent as compared to **5d** (containing 4-chlorophenyl ring). This increased activity of **5c** could be attributed to the presence of bromophenyl ring since its presence makes the molecular slightly more lipophilic as compared to **5d,** containing chlorophenyl ring. Thus, this increased liphophilic character might be responsible for enhanced interaction of compound within active site of enzyme. Consequently, the enhanced ligand protein interaction leads to promising activity of compound **5c** (Fig. 6).

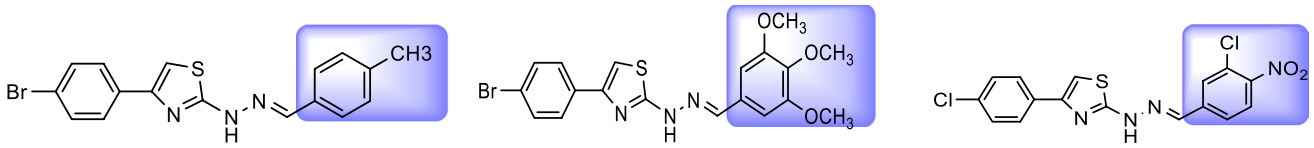

5i (IC_{50} = 110 ± 3 nM) **5l** (IC_{50} = 110 ± 5 nM) **5k** (IC_{50} = 280 ± 10 nM)

Fig. 2 Structure–activity relationship of compounds **5i, 5l** and **5k**

Fig. 3 Structure–activity relationship of compounds **5a** and **5b**

5a (IC_{50} = 330 ± 30 nM) **5b** (IC_{50} = 440 ± 20 nM)

Fig. 4 Structure–activity relationship of compounds **5f, 5h, 5c** and **5g**

5f (IC_{50} = 120 ± 3 nM) **5h** (IC_{50} = 130 ± 2 nM)

5c (IC_{50} = 160 ± 4 nM) **5g** (IC_{50} = 200 ± 2 nM)

Fig. 5 Structure–activity relationship of compounds **5e** and **5f**

5e (IC_{50} = 210 ± 10 nM) **5f** (IC_{50} = 120 ± 3 nM)

Fig. 6 Structure–activity relationship of compounds **5c** and **5d**

5c (IC_{50} = 160 ± 4 nM) **5d** (IC_{50} = 260 ± 20 nM)

Molecular docking studies

Molecular docking studies were executed in order to illustrate the binding mode and interactions of the most significant compounds. The crystalline jack bean (*Canavalia ensiformis*) legume urease enzyme, having a resolution of 1.52 Å, was acquired from the Protein Data Bank (**PDB ID: 4H9M**). The enzyme had a single unique chain of amino acids, pre-docked with its unique ligand acetohydroxamic acid (**HAE**) in the residual sequence of the protein. The ligand binding site of the corresponding enzyme constituted both hydrophobic and hydrophilic amino acids. Acetohydroxamic acid (**HAE**) was bound at the active site displaying both hydrophilic and hydrophobic interactions. The two embedded Ni^{2+} ions (Ni901 and Ni902) unanimously spare a significant role by linking the critical amino acid and ligands. The redocking procedure for the ligand acetohydroxamic acid (HAE) was carried out with the purpose of docking protocol validation, generating multiple docked poses with one pose showing the RMSD value below 1 Å (i.e., 0.6909 Å), hence validating the docking procedure (Fig. 7). The molecular docking study revealed that all the compounds included in study conformed well in the active pocket of the urease enzyme. Moreover, the most promising docked conformations of each compound was evaluated further for binding mode analysis, based on the scores from binding free energy calculation. Afterward, molecular docking of the selected ligands was carried out as discussed below.

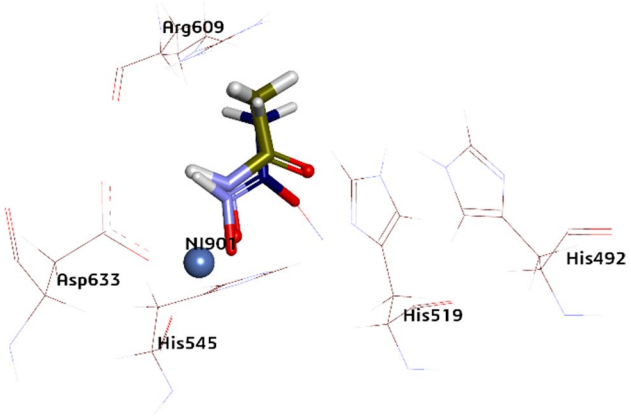

Fig. 7 Ligand acetohydroxamic acid (HAE) with RMSD of 0.6909 Å

Molecular docking of ligands

The docking of compounds was executed by Molecular Operating Environment (MOE 2016.0801) and validated by LeadIT (BioSolveIT GmbH, Germany). Default parameters were used to carry out the docking studies of the selected compounds. Structures **5f**, **5h**, **5i** and **5l** were prepared in ChemDraw, and their energies were minimized in Molecular Operating Environment. For **5f**, the best pose (Fig. 8) is the most suitable pose for the docked compound. Ligand formed hydrogen bonding with Ala440 and Arg609 residues, π–sulfur interaction with His519 and Met637. Glu493 residue showed π–anionic linkage, while Ala636 had π–alkyl interaction with the ligand. Ni^{2+}902 exhibited π–cationic linkage. For **5h**, the best pose (Fig. 9) exhibited hydrogen bonding with His593, π–alkyl interactions with Ala436, Arg439, Ala440, His545, Ala636 and Met637 residues. Arg609 residue showed π–cationic, while Ni^{2+}901 exhibited chemical interactions. For compound **5i**, the best pose (Fig. 10) was chosen as the most suitable pose for the docked compound. The compound exhibited π–alkyl interactions with His409, Arg439, Ala440, Leu523, His545, Ala636 and Met637 residues. Arg609 residue showed π–cationic,

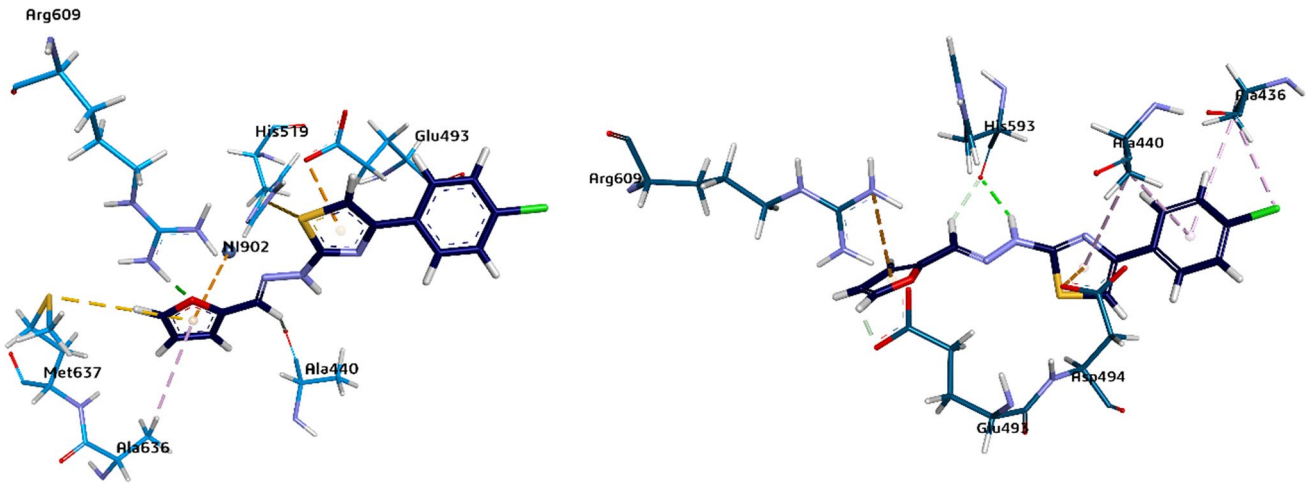

Fig. 8 Compound **5f** docking with protein (left: MOE, right: LeadIT)

while His593 exhibited π–sulfur interactions. Ni^{2+}901 exhibited chemical interactions with the protein. For **5l**, the best pose (Fig. 11) exhibited hydrogen bonding with His407 and His545 residues, π–alkyl interactions with His409, Ala436, Ala440 and His519 residues. Gly550 residue showed π–lone pair interaction with the ligand,

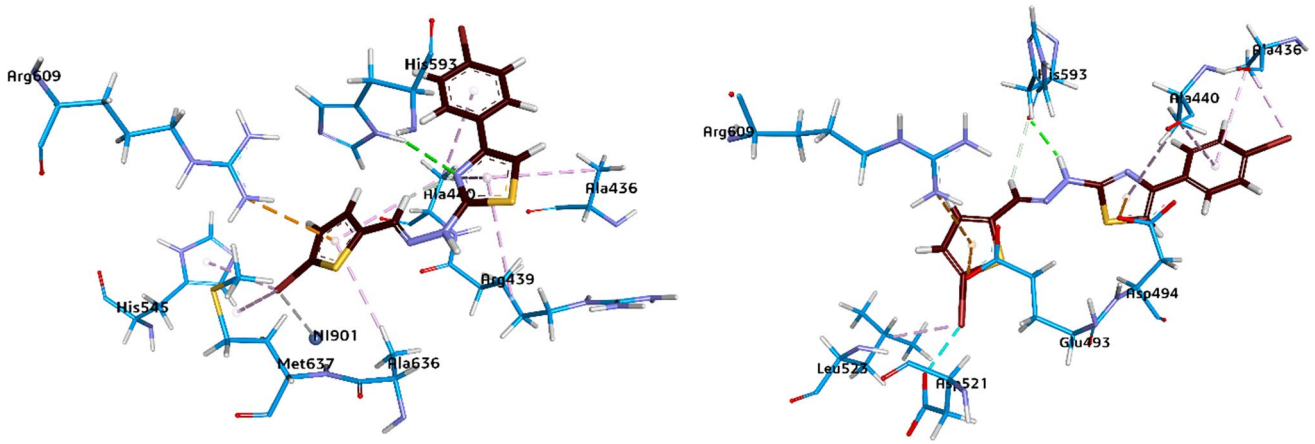

Fig. 9 Compound **5h** docking with protein (left: MOE, right: LeadIT)

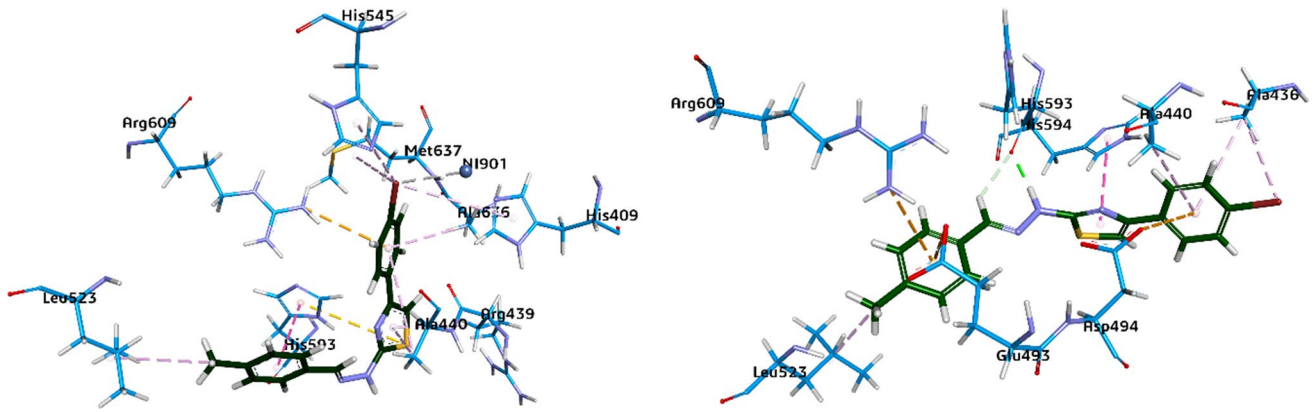

Fig. 10 Compound **5i** docking with protein (left: MOE, right: LeadIT)

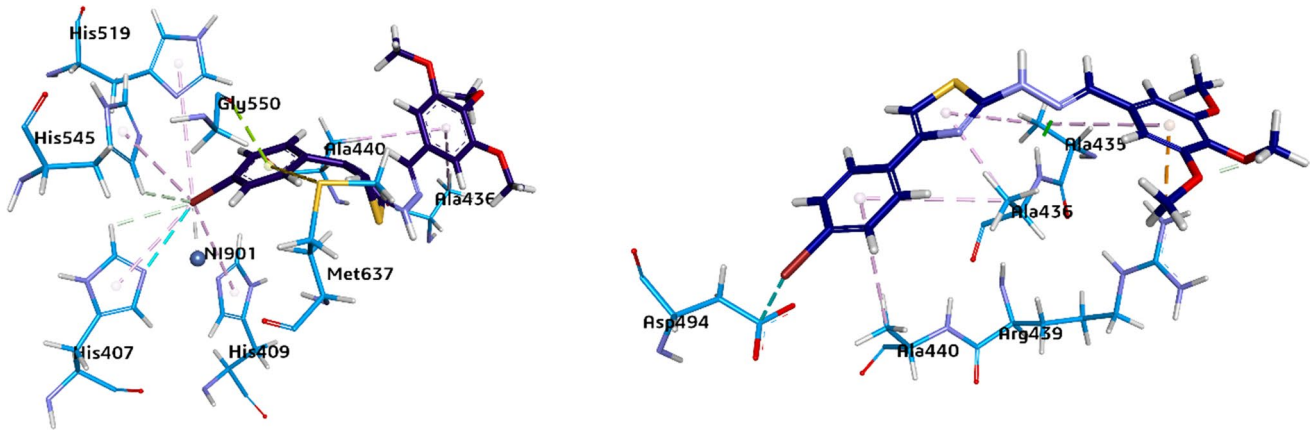

Fig. 11 Compound 5f docking with protein (left: MOE, right: LeadIT)

and Met637 had π–sulfur interactions with the protein. Ni^{2+}901 exhibited chemical interactions with the protein.

Post-docking, the conformations obtained showed good docking score and robust demonstration of in silico inhibition of the urease enzyme. The overall results and correlation concern to molecular docking evaluation were found very promising, revealing that the major criteria for potent inhibition by a ligand is the proximity and linkage to histidine residues tetrad in the urease active pocket (His492, His519, His545 and His593) along with interaction with either of Ni^{2+} (Ni901 and Ni902). The molecular docking results of MOE were validated through LeadIT platform, displaying almost similar interactions.

Experimental

General remarks and instrumentation

All the chemicals were purchased from commercial suppliers (mainly (Sigma-Aldrich Chemical Co., Alfa-Aesar & Merck, etc.). Ethanol was dried using KOH and was stored on 4 Å molecular sieves. TLC was performed on precoated aluminum sheets. Melting points were determined in open glass capillaries using Gallenkamp melting point apparatus (MP-D) and are uncorrected. Infrared spectra (IR) of the compounds were recorded on a Bio-Rad-Excalibur Series Model No. FTS 300 MX spectrophotometer as pure compounds. ^{1}H and ^{13}C-NMR spectra were obtained on a Bruker 300 MHz and 75.5 MHz NMR spectrometer using tetramethyl silane (TMS) as internal reference standard for both ^{1}H and ^{13}C-NMR. Assignments were determined based on unambiguous chemical shift values (δ values). Coupling constants (J values) are given in hertz (Hz), chemical shifts are given in parts per million (ppm), and a number of protons for each signal are also indicated. Abbreviations *s*, *d*, *t*, *q*, *m* were used for singlet, doublet, triplet, quartet and multiplet, respectively. Mass spectra were recorded on Agilent technologies 6890 N gas chromatograph and an inert mass selective detector 5973 mass spectrometer, while the elemental analyses were conducted using a LECO-183 CHNS analyzer.

General experimental procedure for the synthesis of (aryl)methylene)hydrazine-1-carbothioamides (3a–k)

To a stirred solution of hydrazine carbothioamide **1** (2.0 mM) in 25 mL absolute ethanol, suitably substituted aldehydes (**2a–k**) (2.0 mM) along with 1–2 drops of acetic acid were added. The reaction mixture was refluxed for 10–12 h, and progress of reaction was monitored by TLC. Afterward, the reaction mixture was cooled down to room temperature and the solid obtained was filtered and recrystallized from cold methanol to afford the 2-benzylidenehydrazine-1-carbothioamides (**3a–k**).

General experimental procedure for the synthesis of hydrazinyl-1,3-thiazoles (5a–m)

To a stirred solution of appropriate 2-benzylidenehydrazine-1-carbothioamides (**3a–k**) (1.0 mM) in ethanol (25 mL), the respective 4-chloro or 4-bromobenzoyl chloride (**4a–d**) (1.0 mM) was added dropwise during 10 min. The reaction was refluxed for 2 h. Completion of the reaction was monitored by TLC. After completion of the reaction, the reaction mixture was cooled down, and the solid formed was filtered and washed with hexane (30 mL) six–eight times to get pure products as hydrazinyl-1,3-thiazoles **(5a–m).**

(*E*)-2-(2-(4-(benzyloxy)-3-methoxybenzylidene) hydrazinyl)-4-(4-bromophenyl) thiazole (5a)

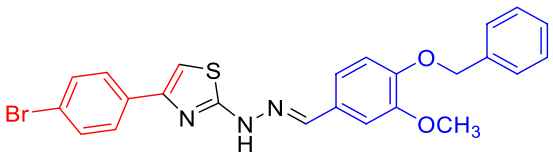

Yield: 80%; Yellow Solid; m.p: 283 °C; R_f = 0.64 (petroleum ether/ethyl acetate, 1:2); **IR** (KBr, ν_{max}/cm^{-1}): 3220 (N–H), 3126 (sp^2C–H), 2960 (sp^3C–H), 1600 (C=N), 1585 (Ar–C=C); **^{1}H-NMR** (DMSO-*d*6, 300 MHz) δ = 12.04 (*s*, 1H, NH), 7.97 (*s*, 1H, HC=N), 7.80 (*d*, 6.3 Hz, 2H, Ar–H), 7.60 (6.3 Hz, 2H, Ar–H), 7.45–7.30 (*m*, 5H, Ar–H), 7.30 (*s*, 1H, CH–thiazole), 7.10 (*dd*, J = 6.6 Hz, 2.1 Hz 2H, Ar–H), 5.13 (*s*, 2H, OCH_2); 3.83 (*s*, 3H, OCH_3); **^{13}C-NMR** (75 MHz, DMSO-*d*6) δ = 168.9, 159.3, 155.0, 149.8, 149.5, 145.0, 142.0, 137.4, 135.9, 131.9, 128.0, 125.9, 120.9, 120.5, 113.9, 109.3, 104.7, 70.4; 55.9; **MS** *m*/*z* (%): 495 (M^+ + 2, 11), 493 (M^+, 48); **Anal.** Calcd. for $C_{24}H_{20}BrN_3O_2S$ (493): C, 58.30; H, 4.08; N, 8.50; S, 6.49: Found: C, 58.28.77, H, 4.10, N, 8.52, S, 6.47%.

(*E*)-1-(4-(benzyloxy)benzylidene)-2-(4-(4-bromophenyl)thiazole-2-yl)hydrazine (5b)

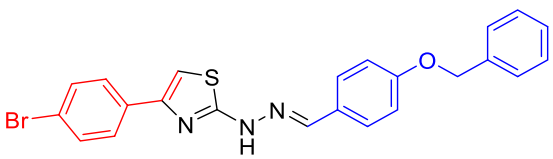

Yield: 70%; Yellow Solid; m.p: 279 °C; R_f = 0.62 (petroleum ether/ethyl acetate, 1:2); **IR** (KBr, ν_{max}/cm^{-1}): 3225

(N–H), 3122 (sp^2C–H), 2964 (sp^3C–H), 1605 (C=N), 1595 (Ar–C=C); **^{1}H-NMR**:(DMSO-*d*6, 300 MHz) $\delta = 11.88$ (1H, *s*, broad, NH), *d* 8.0 (*s*, 1H, HC=N), 7.40 (*d*, 5.4 Hz, 2H, Ar–H), 7.30 (*m*, 5H, Ar–H), 7.12 (*d*, 2H, $J = 8.1$ Hz, Ar–H), 7.29 (*d*, 2H, $J = 8.1$ Hz, Ar–H), 7.20 (*s*, 1H, Ar–H), 7.0 (*d*, 6.6 Hz, 2H, Ar–H), 5.11 (*s*, 2H, OCH_2); **^{13}C-NMR** (75 MHz, DMSO-*d*6) $\delta = 171.6$, 161.2, 150.1, 143.2, 136.5, 134.2, 131.0, 130.1, 129.1, 128.7, 127.5, 127.0, 125.5, 126.1, 114.2, 105.1, 70.7; **MS** *m*/*z* (%): 465 ($M^+ + 2$, 13), 463 (M^+, 55). **Anal.** Calcd. For $C_{23}H_{18}BrN_3OS$ (463): C, 59.49; H, 3.91; N, 9.05; S, 6.90. Found: C, 59.47; H, 3.93; N, 9.03; S, 6.92%.

(*E*)-1-(4-(4-bromophenyl)thiazole-2-yl)-2-(pyridin-3-ylmethylene)hydrazine (5c)

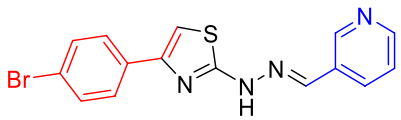

Yield: 75%; Yellow Solid; m.p: 269 °C; $R_f = 0.68$ (petroleum ether/ethyl acetate, 1:2); **IR** (KBr, ν_{max}/cm^{-1}): 3230 (N–H), 3130 (sp^2C–H), 1608 (C=N), 1583 (Ar–C=C); **^{1}H-NMR** (DMSO-*d*6, 300 MHz) $\delta = 11.03$ (*s*, 1H, NH), 9.03 (*s*, 1H, Ar–H), 8.77 (*d*, $J = 7.5$, 1.3 Hz, 1H, Ar–H), 8.58 (*d*, $J = 1.3$ Hz, 1H, Ar–H), 8.16 (*s*, 1H, HC=N), 7.92 (t, $J = 7.5$ Hz, 1H, Ar–H), 7.90 (*d*, 2H, $J = 8.1$ Hz, Ar–H), 7.83 (*d*, 2H, $J = 8.1$ Hz, Ar–H), 7.50 (*s*, 1H, thiazole); **^{13}C-NMR** (75 MHz, DMSO-*d*6) $\delta = 168.3$, 149.9, 146.6, 143.1, 138.1, 137.2, 136.5, 134.2, 132.0, 128.0, 126.6, 121.1, 105.9; **MS** *m*/*z* (%): 360 ($M^+ + 2$, 13), 358 (M^+, 50); **Anal.** Calcd. For $C_{15}H_{11}BrN_4S$ (358): C, 50.15; H, 3.09; N, 15.60; S, 8.93 Found: C, 50.13; H, 3.11; N, 15.62; S, 8.91%.

(*E*)-1-(4-(4-chlorophenyl)thiazol-2-yl)-2-(pyridin-3-ylmethylene)hydrazine (5d)

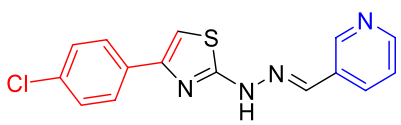

Yield: 73%; Yellow Solid; m.p: 278 °C; $R_f = 0.62$ (petroleum ether/ethyl acetate, 1:2); **IR** (KBr, ν_{max}/cm^{-1}): 3320 (N–H), 3146 (sp^2CH), 1590 (C=N), 1580 (Ar–C=C); **^{1}H-NMR** (DMSO-*d*6, 300 MHz) $\delta = 11.66$ (*s*, 1H, NH), 8.91 (*dd*, $J = 7.5$, 1.3 Hz, 1H, Ar–H), 8.57 (*d*, $J = 1.3$ Hz, 1H, Ar–H), 8.21 (*dt*, $J = 7.5$, 1.4 Hz, 1H, Ar–H), 8.13 (*s*, 1H, HC=N), 7.45 (t, $J = 7.5$ Hz, 1H, Ar–H), 7.8 (*d*, 6.3 Hz, 2H, Ar–H), 7.6 (*d* 6.3 Hz, 2H, Ar–H), 7.1 (*s*, 1H, thiazole): **^{13}C-NMR** (75 MHz, DMSO-*d*6) $\delta = 171.7$, 159.3, 155.4, 144.1, 140.5, 137.1, 134.1, 131.1, 129.6, 128.7, 126.1, 121.2, 105.4; **MS** *m*/*z* (%): 316 ($M^+ + 2$, 10), 314 (M^+, 48). **Anal.** Calcd. For $C_{15}H_{11}ClN_4S$ (314): C, 57.23; H, 3.52; N, 17.80; S, 10.19%. Found: C, 57.21; H, 3.54; N, 17.78; S, 10.21%.

(*E*)-1-(4-(4-bromophenyl)thiazole-2-yl)-2-(furan-2-ylmethylene)hydrazine (5e)

Yield: 77%; Yellow Solid; m.p: 258 °C; $R_f = 0.56$ (petroleum ether/ethyl acetate, 1:2); **IR** (KBr, ν_{max}/cm^{-1}): 3228 (N–H), 3124 (sp^2C–H), 1603 (C=N), 1595 (Ar–C=C); **^{1}H-NMR** (DMSO-*d*6, 300 MHz) $\delta = 11.51$ (*s*, 1H, NH), 8.2 (*s*, 1H, CH=N), 7.9 (*s*, 1H thiazole), 7.8 (*dd*, $J = 7.5$, 1.6 Hz, 1H, Ar–H), 7.6 (t, $J = 7.4$ Hz, 1H Ar–H), (*d*, 2H, $J = 7.7$ Hz, Ar–H), 7.43 (*d*, 2H, $J = 7.7$ Hz, Ar–H); **^{13}C-NMR** (75 MHz, DMSO-*d*6) $\delta = 173.7$, 162.3, 152.4, 144.1, 134.5, 129.7, 128.6, 126.0, 121.3, 118, 115, 105.5; **MS** *m*/*z* (%): 349 ($M^+ + 4$, 30), 347 ($M^+ + 2$, 12), 345 (M^+, 60); **Anal.** Calcd. For $C_{14}H_{10}BrN_3OS$ (346): C, 48.29; H, 2.89; N, 12.07; S, 9.21%. Found: C, 48.31; H, 2.79; N, 12.05; S, 9.23%.

(*E*)-4-(4-chlorophenyl)-2-(2-(furan-2-ylmethylene) hydrazinyl) thiazole (5f)

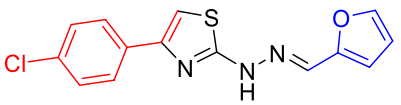

Yield: 77%; Brown Solid; m.p: 298 °C; $R_f = 0.56$ (petroleum ether/ethyl acetate, 1:2); **IR** (KBr, ν_{max}/cm^{-1}): 3349 (N–H), 3135 (sp^2C–H), 1570 (C=N), 1560 (Ar–C=C); **^{1}H-NMR** (DMSO-*d*6, 300 MHz) $\delta = 11.51$ (*s*, 1H, NH), 8.2 (*s*, 1H, CH=N), 7.8 (*dd*, $J = 7.5$, 1.6 Hz, 2H, Ar–H), 7.6 (t, $J = 7.4$ Hz, 1H), 7.4 (*d*, 6.3 Hz, 2H), 7.3 (*s*, 1H, thiazole), 6.9 (6.3 Hz, 2H, Ar–H); **^{13}C-NMR** (75 MHz, DMSO-*d*6) $\delta = 173.7$, 162.3, 152.4, 144.1, 134.5, 129.7, 128.6, 126.0, 121.3, 118.1, 115.0, 105.5; **MS** *m*/*z* (%): 303 (M^+, 40); **Anal.** Calcd. For $C_{14}H_{10}ClN_3OS$ (303): C, 55.35; H, 3.32; N, 13.83; S, 10.56%. Found: C, 55.33; H, 3.34; N, 13.82; S, 10.57%.

(*E*)-1-((5-bromo-1*H*-pyrrol-2-yl) methylene)-2-(4-(4-bromophenyl)thiazole-2-yl) hydrazine (5g)

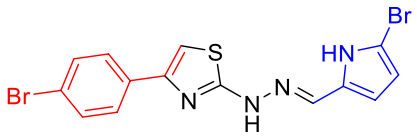

Yield: 75%; Brown Solid; m.p: 302 °C; R_f = 0.66 (petroleum ether/ethyl acetate, 1:2); **IR** (KBr, ν_{max}/cm^{-1}): 3250 (N–H), 3166 (sp^2C–H), 1662 (C=N), 1640 (Ar–C=C); **^{1}H-NMR** (DMSO-*d*6, 300 MHz) δ = 11.9 (*s*, 1H, NH), 11.3 (*s*, 1H, NH), 7.9 (*s*, 1H, CH=N), 7.7 (*dd*, 2H, Ar–H), 7.6 (*dd*, 2H, Ar–H), 7.2 (*s*, 1H, thiazole), 6.7 (*d*, *J* = 8.2 Hz, 1H, Ar–H), 6.5 (*d*, *J* = 8.2 Hz, 1H, Ar–H); **^{13}C-NMR** (75 MHz, DMSO-*d*6) δ = 171.5, 161.6, 152.4, 149.1, 144.5, 132.7, 128.6, 126.0, 1191.3, 117.0, 115.1, 104.5; **MS** *m*/*z* (%): 426 (M^+ + 2, 10), 424 (M^+, 48); **Anal.** Calcd. For $C_{14}H_{10}Br_2N_4S$ (424): C, 39.46; H, 2.37; N, 13.15; S, 7.52%. Found: C, 39.47; H, 2.35; N, 13.13; S, 7.52%.

(*E*)-1-(4-(4-bromophenyl)thiazole-2-yl)-2-((5-bromothiophen-2-yl)methylene) hydrazine (5h)

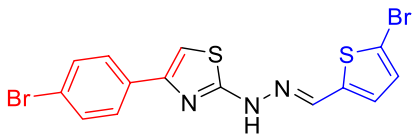

Yield: 75%; Yellow Solid; m.p: 243 °C; R_f: 0.42 (petroleum ether/ethyl acetate, 3:2): **IR** (KBr, ν_{max}/cm^{-1}): 3264 (N–H), 3126 (sp^2C–H), 1609 (C=N), 1587 (Ar–C=C), 1080 (C=S); **^{1}H-NMR** (300 MHz, DMSO-*d*6) δ = 10.42 (*s*, 1H, NH), 7.63 (*s*, 1H, CH=N), 6.68 – 6.65 (*m*, 2H, Ar–H). 7.52 (*s*, 1H), 7.4 (*d*, 6.3 Hz, 2H), 7.2 (6.3 Hz, 2H); **^{13}C-NMR** (75 MHz, DMSO-*d*6) δ = 171.4, 149.6, 148.8, 135.6, 131.2, 130.6, 129.5, 128.6, 117.1, 106.5; **MS** *m*/*z* (%): 443 (M^+ + 2, 14), 441 (M^+, 50); **Anal.** Calcd. For $C_{14}H_9Br_2N_3S_2$ (441): C, 37.94; H, 2.05; N, 9.48; S, 14.47%. Found: C, 37.92; H, 2.07; N, 9.46; S, 14.49%.

(*E*)-4-(4-bromophenyl)-2-(2-(4-methylbenzylidene) hydrazinyl) thiazole (5i)

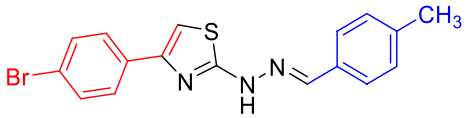

Yield: 76%; Yellow Solid; m.p: 287 °C; R_f = 0.59 (petroleum ether/ethyl acetate, 1:2); **IR** (KBr ν_{max}/cm^{-1}): 3240 (N–H), 3176 (sp^2C–H), 1632 (C=N), 1620 (Ar–C=C); **^{1}H-NMR** (DMSO-*d*6, 300 MHz) δ = 10.42 (*s*, 1H, NH), 7.63 (*s*, 1H, CH=N), 7.29 (*d*, 2H, *J* = 8.0 Hz, Ar–H), 7.21 (*d*, 2H, *J* = 8.1 Hz, Ar–H), **7.52 (*s*, 1H**), 7.4 (*d*, 6.3 Hz, 2H), 7.2 (*s*, 1H, thiazole), 2.36 (*s*, 3H, CH_3); **^{13}C-NMR** (75 MHz, DMSO-*d*6) δ = 171.7, 150.3, 145.4, 143.1, 134.5, 133.1, 132.1, 131.0, 129.7, 129.6, 126.0, 125.5, 104.4; **MS** *m*/*z* (%): 373 (M^+ + 2, 8), 371 (M^+, 38); **Anal.** Calcd. For $C_{17}H_{14}BrN_3S$ (371): C, 54.85; H, 3.79; N, 11.29; S, 8.61%. Found: C, 54.83; H, 3.81; N, 11.27; S, 8.63%.

(*E*)-4-(4-bromophenyl)-2-(2-(2-fluorobenzylidene) hydrazinyl) thiazole (5j)

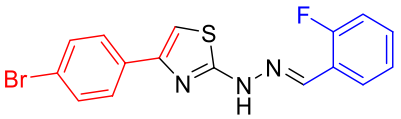

Yield: 86%; Brown Solid; m.p: 299 °C; R_f = 0.64 (petroleum ether/ethyl acetate, 1:2); **IR** (KBr, ν_{max}/cm^{-1}): 3248 (N–H), 3170 (sp^2C–H), 1642 (C=N), 1626 (Ar–C=C); **^{1}H-NMR** (DMSO-*d*6, 300 MHz) δ = 11.56 (*s*, 1H, NH), 7.45 (*s*, 1H, CH=N), 8.27–7.19 (*m*, 4H, Ar–H), 7.42 (*d*, 2H, *J* = 8.2 Hz, Ar–H), 7.41 (*d*, 2H, *J* = 8.2 Hz, Ar–H), 7.21 (*s*, 1H, thiazole); **^{13}C-NMR** (75 MHz, DMSO-*d*6) δ = 175.7, 165.3, 153.8, 149.0, 139.1, 136.1, 134.1, 133.2, 132.2, 129.7, 128.6, 127.0, 126.3, 106.4; **MS** *m*/*z* (%): 375 (M^+, 55); **Anal.** Calcd. For $C_{16}H_{11}BrFN_3S$ (375): C, 51.08; H, 2.95; N, 11.17; S, 8.52%. Found: C, C, 51.09; H, 2.94; N, 11.19; S, 8.50%.

(*E*)-1-(3-chloro-4-nitrobenzylidene)-2-(4-(4-chlorophenyl) thiazole-2-yl) hydrazine (5k)

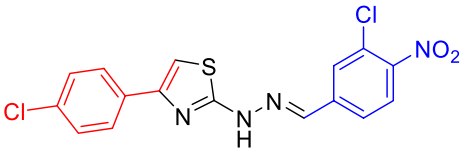

Yield: 76%; Yellow Solid; m.p: 287 °C; R_f = 0.59 (petroleum ether/ethyl acetate, 1:2); **IR** (KBr, ν_{max}/cm^{-1}): 3290 (N–H), 3156 (sp^2C–H), 1570 (C=N), 1560 (Ar–C=C); **^{1}H-NMR** (DMSO-*d*6, 300 MHz) δ = 10.11 (*s*, 1H, NH), 8.43 (*s*, 1H, CH=N), 6.64–7.97 (*m*, 3H, Ar–H), 7.16 (*d*, 2H, *J* = 8.1 Hz, Ar–H), 7.54 (*d*, 2H, *J* = 8.1 Hz, Ar–H), 7.4 (*s*, 1H, thiazole); **^{13}C-NMR** (75 MHz, DMSO-*d*6) δ = 168.4, 149.8, 148.4, 138.4, 135.5, 132.6, 132.5, 130.9, 129.1, 127.7, 125.1, 123.2. 105.5; **MS** *m/z* (%): 394 (M^+ + 2, 12), 492 (M^+, 40); **Anal.** Calcd. For $C_{16}H_{10}C_{l2}N_4O_2S$ (392): C, 48.87; H, 2.56; N, 14.25; S, 8.15%. Found: C, 48.85; H, 2.58; N, 14.24; S, 8.16%.

(*E*)-1-(3,4,5-trimethoxybenzylidene)-2-(4-(4-bromophenyl)thiazole-2-yl)hydrazine (5l)

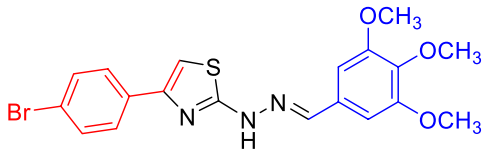

Yield: 87%; Yellow Solid; m.p: 300 °C; R_f = 0.74 (petroleum ether/ethyl acetate, 1:2); **IR** (KBr, ν_{max}/cm^{-1}): 3320 (N–H), 1585 (C=N), 1625(Ar–C=C), 1090 (C–S); **^{1}H-NMR** (DMSO-*d*6, 300 MHz) δ = 10.4 (*s*, 1H, NH), 7.97 (*s*, 1H, CH=N), 7.39 (*d*, 2H, *J* = 8.1 Hz, Ar–H), 7.35 (*d*, 2H, *J* = 8.1 Hz, Ar–H), 7.1 (*s*, 1H, thiazole), 6.89 (*s*, 1H, Ar–H), 6.85 (*s*, 1H, Ar–H), 3.8 (*s*, 6H, $2^{\times}OCH_3$), 3.4 (*s*, 3H, OCH_3); **^{13}C-NMR** (75 MHz, DMSO-*d*6) δ = 173.7, 166.3, 152.8, 149.1, 147.2, 136.1, 134.1, 133, 132.2, 128.6, 126.3, 123, 105.4, 104.5 65, 60; **MS** *m/z* (%): 449 (M^+ + 2, 10), 447 (M^+, 55); **Anal.** Calcd. For $C_{19}H_{18}BrN_3O_3S$ (447): C, 50.90; H, 4.05; N, 9.37; S, 7.15; O, 22.63%. Found: C, 50.92; H, 4.03; N, 9.35; S, 7.17%.

(*E*)-4-(4-bromophenyl)-2-(2-(pyren-1-ylmethylene) hydrazinyl) thiazole (5m)

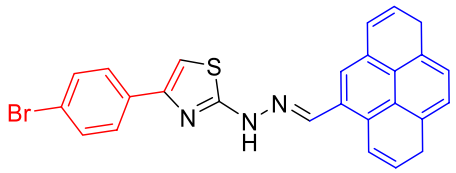

Yield: 65%; Yellow Solid; m.p: 282 °C; R_f = 0.51(petroleum ether/ethyl acetate, 1:2); **IR** (KBr, ν_{max}/cm^{-1}): 3220 (N–H), 1580 (C=N), 1605(Ar–C=C), 1080 (C–S); **^{1}H-NMR** (DMSO-*d*6, 300 MHz) δ = 10.4 (*s*, 1H, NH), 8.2–8.5 (*m*, 3H, Ar–H), 7.97 (*s*, 1H, CH=N), 7.94–7.92 (*m*, 2H, Ar–H), 7.7–7.62 (*m*, 4H, Ar–H), 7.8 (*d*, 6.1 Hz, 2H, Ar–H), 7.6 (*d*, 6.1 Hz, 2H, Ar–H), 7.1 (*s*, 1H, thiazole); **^{13}C-NMR** (75 MHz) δ = 171.0, 144.2, (C=N), 150.5 (C=C), 145.3 (Ar); 143.1 (Ar), 140.2 (Ar), 137.5 (Ar), 134.5 (Ar), 133.3 (Ar), 132.5 (Ar), 130.6 (Ar), 132.5, 133.1, 130.5, 126.6, 129.5, 127, 123.5, (Ar), 105; **MS** *m/z* (%): 483 (M^+ M^+, 45); **Anal.** Calcd. For $C_{26}H_{16}BrN_3S$ (481): C, 64.74; H, 3.34; N, 8.71; S, 6.65%. Found: C, 64.72; H, 3.36; N, 8.70; S, 6.66%.

Urease inhibition assay

The assay was performed as described by Weatherburn with slight modifications [30]. The assay was conducted by adding 10 µL of compound solution and 10 µL of enzyme (5 U/mL) to 40 µL of assay buffer (urea 100 mM, EDTA 1 mM, K_2HPO_4 0.01 M and $LiCl_2$ 0.01 M, pH 8.2). The reaction mixture was incubated for 10 min at 37 °C. Then, 40 µL of phenol reagent [phenol (1% w/v) and sodium nitroprusside (0.005% w/v)] and 40 µL of alkali reagent [NaOH (0.5% w/v) and NaOCl (0.1%)] was added and mixture was again incubated for 30 min. Subsequently, absorbance was measured at 625 nm using microplate reader (OMEGA® Flow Star Microplate Germany). The concentration–response curves were fitted, and IC_{50} values were calculated by using GraphPad PRISM 5.0 software (GraphPad, San Diego, California, USA). Thiourea was used as standard inhibitor. All the experiments were performed in triplicate.

Molecular modeling studies

Crystalline structure of jack bean urease enzyme was downloaded from the Protein Data Bank (PDB ID: 4H9M) [31]. Structures of ligands (**5i**, **5l**, **5h** and **5f**) were prepared using ChemDraw and optimized through Molecular Operating Environment (MOE 2019.0201) [32]. Molecular docking was performed by adopting MOE 2019.0201 protocol. Compounds were redocked using LeatIT [33] platform to validate the initial docking of MOE. From docked conformations, the most favorable pose with better binding free energy was selected. Docked conformations were visualized using BIOVIA Discovery Studio 2019 [34].

Conclusions

In summary, a diverse series of new 4-aryl-2-hydrazinyl-1,3-thiazoles (**5a–m**), with structural variation at nitrogen atom of hydrazine, was synthesized and evaluated for anti-urease inhibition potential. The in vitro analysis against urease activity revealed that most of the synthesized compounds were active against urease catalysis compared to the standard inhibitor, i.e., thiourea (490 ± 10 nM). A detailed SAR indicated that compounds substituted with electron donating groups were more active compared to the others **5i** (110 ± 3 nM) and **5l** (110 ± 5 nM). Hetero-aromatic rings at nitrogen of hydrazine showed intermediate inhibition, while least inhibition was indicated by benzyloxy substituents. The molecular docking studies on four most active compounds (**5i, 5l, 5h** and **5f**) were performed against legume Jack bean (*Canavalia ensiformis*) urease enzyme with Protein Data Bank (PDB) ID: 4H9M to rationalize the experimental activity, and it was observed that the in silico results for the selected compounds match well the results predicted by the in vitro outcomes. Molecular docking also suggested that the selected compounds show significant interactions within the active pocket of the urease enzyme and demonstrate convincing inhibition capacity for the enzyme urease.

Acknowledgements A.S. is grateful to Alexander von Humboldt Foundation Germany, for a Gerog Forster Post-doctoral fellowship. J.I. is thankful to the Higher Education Commission of Pakistan for the financial support through Project No. Ph-V-MG-3/Peridot/R&D/HEC/2019.

References

1. Yao M, Tu W, Chen X, Zhan CG (2013) Reaction pathways and free energy profiles for spontaneous hydrolysis of urea and tetramethylurea: unexpected substituent effects. Org Biomol Chem 11:7605. https://doi.org/10.1039/c3ob41055b
2. Krajewska B (2009) Ureases I. Functional, catalytic and kinetic properties: a review. J Mol Catal B Enzym 59:21. https://doi.org/10.1016/j.molcatb.2009.01.003
3. Callahan BP, Yuan Y, Wolfenden R (2005) The burden borne by urease. J Am Chem Soc 10:10829. https://doi.org/10.1021/ja0525399
4. Maroney MJ, Ciurli S (2014) Nonredox nickel enzymes. Chem Rev 23:4228. https://doi.org/10.1021/cr4004488
5. Shehzadi SA, Khan I, Saeed A, Larik FA, Channar PA, Hassan M, Raza H, Abbas Q, Seo SY (2019) One-pot four-component synthesis of thiazolidin-2-imines using CuI/ZnII dual catalysis: a new class of acetylcholinesterase inhibitors. Bioorg Chem 84:528. https://doi.org/10.1016/j.bioorg.2018.12.002
6. Boer JL, Mulrooney SB, Hausinger RP (2014) Nickel-dependent metalloenzymes. Arch Biochem Biophys 544:152. https://doi.org/10.1016/j.abb.2013.09.002
7. Mobley HLT (2001) Urease. In: Mobley HLT, Mendz GL, Stuart L (eds) Helicobacter pylori: physiology and genetics. American Society of Microbiology Press, Hague
8. Hassan ST, Šudomová M (2017) The development of urease inhibitors: what opportunities exist for better treatment of *Helicobacter pylori* infection in children. Children 4:2
9. Krajewska B (2016) A combined temperature-pH study of urease kinetics. Assigning pKa values to ionizable groups of the active site involved in the catalytic reaction. J Mol Catal 124:76. https://doi.org/10.1371/journal.ppat.1004472
10. Mora D, Arioli S (2014) Microbial urease in health and disease. PLoS Pathog 10:1004472. https://doi.org/10.1371/journal.ppat.1004472
11. Hausinger RP, Karplus PA (2006) Urease. In: handbook on metalloproteins. Clin Microbiol Rev 19:613. https://doi.org/10.1371/journal.ppat.1004472
12. Amtul Z, Rahman A, Siddiqui R, Choudhary M (2002) Chemistry and mechanism of urease inhibition. Curr Med Chem 9:1323. https://doi.org/10.2174/0929867023369853
13. Rego YF, Queiroz MP, Brito TO, Carvalho PG, de Queiroz VT, de Fátima F, Jr Macedo (2018) A review on the development of urease inhibitors as antimicrobial agents against pathogenic bacteria. J Adv Res 13:69. https://doi.org/10.1016/j.jare.2018.05.003
14. Upadhyay LSB (2012) Urease inhibitors: a review. Ind J Biotechnol 11:381
15. Macegoniuk K (2013) Inhibitors of bacterial and plants urease. A review. Folia Biol Oecol 9:9. https://doi.org/10.2478/fobio-2013-0004
16. Modolo LV, de Souza AX, Horta LP, Araujo DP, de Fátima A (2015) An overview on the potential of natural products as ureases inhibitors: a review. J Adv Res 6:35. https://doi.org/10.1016/j.jare.2014.09.001
17. Kosikowska P, Berlicki Ł (2011) Urease inhibitors as potential drugs for gastric and urinary tract infections: a patent review. Expert Opin Ther Pat 21:945. https://doi.org/10.1517/13543776.2011.574615
18. Kafarski P, Talma M (2018) Recent advances in design of new urease inhibitors: a review. J Adv Res 13:101. https://doi.org/10.1016/j.jare.2018.01.007
19. Bektaş H, Ceylan S, Demirbaş N, Karaoğlu SA, Sökmen BB (2013) Antimicrobial and antiurease activities of newly synthesized morpholine derivatives containing an azole nucleus. Med Chem Res 22:3629. https://doi.org/10.1007/s00044-012-0318-1
20. Taha M, Ismail NH, Imran S, Wadood A, Rahim F, Khan KM, Riaz M (2016) Hybrid benzothiazole analogs as antiurease agent: synthesis and molecular docking studies. Bioorg Chem 66:80. https://doi.org/10.1016/j.bioorg.2016.03.010
21. Saeed A, Channar PA, Shabir G, Larik FA (2006) Green synthesis, characterization and electrochemical behavior of new

thiazole based coumarinyl scaffolds. J Fluoresc 26:1067. https://doi.org/10.1007/s10895-016-1795-2
22. Das J, Chen P, Norris D, Padmanabha R, Lin J, Moquin RV, Shen Z, Cook LS, Doweyko AM, Pitt S, Pang S (2006) 2-aminothiazole as a novel kinase inhibitor template. Structure–activity relationship studies toward the discovery of N-(2-chloro-6-methylphenyl)-2-[[6-[4-(2-hydroxyethyl)-1-piperazinyl)]-2-methyl-4-pyrimidinyl]amino)]-1,3-thiazole-5-carboxamide (dasatinib, BMS-354825) as a potent pan-Src kinase inhibitor. J Med Chem 49:6819. https://doi.org/10.1021/jm060727j
23. Rouf A, Tanyeli CC (2015) Bioactive thaizole and benzothiazole derivatives. Eur J Med Chem 975:911
24. Chun MW, Kim MJ, Shin JH, Jeong LS (2005) Synthesis of 3′-deoxy-3′-*c*-hydroxymethyl analogues of tiazofurin and ribavirin. Nucleosides Nucleotides Nucleic Acids 24:975. https://doi.org/10.1081/NCN-200059338
25. Grozav A, Găină LI, Pileczki V, Crisan O, Dumitrescu LS, Therrien B, Zaharia V, Neagoe IB (2014) The synthesis and antiproliferative activities of new arylidene-hydrazinyl-thiazole derivatives. Int J Mol Sci 15:22059. https://doi.org/10.3390/ijms151222059
26. Rahman FSA, Yusufzai SK, Osman H, Mohamad D (2016) Synthesis, characterisation and cytotoxicity activity of thiazole substitution of coumarin derivatives (characterisation of coumarin derivatives). J Phys Sci 27:77
27. Yusufzai SK, Osman H, Khan MS, Mohamad S, Sulaiman O, Parumasivam T, Gansau JZ, Noviany NJ (2017) Design, characterization, in vitro antibacterial, antitubercular evaluation and structure–activity relationships of new hydrazinyl thiazolyl coumarin derivatives. Med Chem Res 26:1139. https://doi.org/10.1007/s00044-017-1820-2
28. Makam P, Kankanala R, Prakash A, Kannan T (2013) 2-(2-Hydrazinyl)thiazole derivatives: design, synthesis and in vitro antimycobacterial studies. Eur J Med Chem 69:564. https://doi.org/10.1016/j.ejmech.2013.08.054
29. Osorio E, Bravo K, Cardona W, Yepes A, Osorio EH, Coa JC (2019) Antiaging activity, molecular docking, and prediction of percutaneous absorption parameters of quinoline–hydrazone hybrids. Med Chem Res 28:1959. https://doi.org/10.1007/s00044-019-02427-0
30. Weatherburn MW (1967) Phenol-hypochlorite reaction for determination of ammonia. Anal Chem 39:971. https://doi.org/10.1021/ac60252a045
31. Begum A, Choudhary MI, Betzel C (2012) The first Jack bean urease (*Canavalia ensiformis*) complex obtained at 1.52 resolution. https://doi.org/10.2210/pdb4h9m/pdb
32. Chemical Computing Group's Molecular Operating Environment (MOE) MOE 2019.0201
33. LeadIT Version 2.3.2 (2017) BioSolveIT GmbH, Sankt Augustin, Germany. www.biosolveit.de/LeadIT
34. BIOVIA Discovery Studio Client v19.1.0.18287